Apical sorting of beta-secretase limits amyloid beta-peptide production

Anja Capell, Liane Meyn, Regina Fluhrer, David B. Teplow, Jochen Walter, Christian Haass

Angaben zur Veröffentlichung / Publication details:

Capell, Anja, Liane Meyn, Regina Fluhrer, David B. Teplow, Jochen Walter, and Christian Haass. 2002. "Apical sorting of beta-secretase limits amyloid beta-peptide production." *Journal of Biological Chemistry* 277 (7): 5637–43. https://doi.org/10.1074/jbc.m109119200.

THE JOURNAL OF BIOLOGICAL CHEMISTRY
Vol. 277, No. 7, Issue of February 15, pp. 5637–5643, 2002
Printed in U.S.A.

Apical Sorting of β-Secretase Limits Amyloid β-Peptide Production*

Received for publication, September 21, 2001, and in revised form, November 29, 2001
Published, JBC Papers in Press, December 6, 2001, DOI 10.1074/jbc.M109119200

Anja Capell‡, Liane Meyn‡, Regina Fluhrer‡, David B. Teplow§, Jochen Walter‡, and Christian Haass‡¶

From the ‡Adolf Butenandt-Institute, Department of Biochemistry, Laboratory for Alzheimer's and Parkinson's Disease Research, Schillerstrasse 44, Ludwig-Maximilians-University, Munich 80336, Germany and the §Department of Neurology, Harvard Medical School, and Center for Neurologic Diseases, Brigham and Women's Hospital, Boston, Massachusetts 02115

Polarized cells such as neurons and endothelial cells appear to be involved in two invariant pathological features of Alzheimer's disease pathology, namely the formation of senile plaques and cerebral amyloid angiopathy. This implicates polarized sorting mechanisms in the production and accumulation of amyloid β-peptide (Aβ). We have now studied polarized sorting of β-secretase (BACE) in Madin-Darby canine kidney (MDCK) cells. The majority of BACE is sorted to the apical surface of MDCK cells where very little β-amyloid precursor protein (βAPP) is observed, because βAPP undergoes basolateral sorting. Consistent with the usage of similar mechanisms for polarized sorting, BACE was also found to be targeted to axons of hippocampal neurons. The remaining basolaterally sorted BACE competes with the highly polarized basolateral α-secretase activity. Therefore, substantial amounts of BACE are targeted away from βAPP to a non-amyloidogenic compartment, a cellular mechanism that limits Aβ generation. In addition, no α-secretase activity was observed on the apical side whereas γ-secretase activity is observed on the basolateral and the apical side. Consistent with this finding, substantial amounts of Aβ can be produced apically upon missorting of βAPP to the apical surface. These data demonstrate that Aβ production is limited in polarized cells by differential targeting of BACE and its substrate βAPP. Moreover, our findings suggest that βAPP may not be a major physiological substrate of BACE.

Proteolytic enzymes called secretases play a pivotal role in the generation of amyloid β-peptide (Aβ[1]), the major component of the Alzheimer's disease (AD)-defining senile plaques and microvascular deposits (1). β-Secretase (BACE), a membrane-bound aspartyl protease (2–6), is responsible for the cleavage at the N terminus of the Aβ domain at Asp-1 and Glu-11. This heterogenous cleavage results in the generation of membrane-bound βAPP C-terminal fragments (βAPP CTFs), which are the immediate precursors for Aβ generation (1), and in the secretion of the truncated ectodomain of βAPP (7). γ-Secretase activity, which critically requires the presenilins PS1/PS2 (8–15), mediates the cleavage at the C terminus of the Aβ domain. This final proteolytic event results in the secretion of Aβ into biological fluids (1) and the liberation of the C-terminal domain of βAPP into the cytoplasm (16). A third secretase, the α-secretase, prevents Aβ generation by cleaving in the middle of the Aβ-domain. The α-secretase activity is associated with three members (ADAM 9, 10, and 17) of the ADAM (a disintegrin and metalloprotease) family (17–19) and generates the secreted ectodomain of βAPP (APPsα). The remaining C-terminal stub is processed by γ-secretase, which results in the secretion of p3 (1).

Polarized cells are intimately associated with two invariant pathological features of AD pathology, namely the formation of senile plaques and the cerebral amyloid angiopathy. This suggests that polarized sorting mechanisms may be involved in the production and accumulation of Aβ. As a model system to study polarized sorting of βAPP and the three secretase activities, we used the well characterized Madin-Darby canine kidney (MDCK) cells, because they allow the generation of stably transfected cell lines with moderate expression levels and appear to use similar mechanisms for polarized sorting as neuronal cells (20). Moreover, experiments on polarized sorting of βAPP in this cell line provided first evidence for the cellular mechanism underlying the enhanced Aβ production caused by the Swedish mutation (21, 22), thus demonstrating the relevance of MDCK cells for studies on βAPP processing. βAPP is known to undergo polarized sorting in MDCK cells (21–24) as well as in neurons (25, 26). In MDCK cells the βAPP holoprotein and its proteolytic products are predominantly targeted to the basolateral side. A targeting signal containing a tyrosine within the cytoplasmic domain of βAPP is required for polarized sorting of membrane-associated βAPP (24). Deletion of the cytoplasmic sorting signal of βAPP leads to an equal surface distribution of membrane-associated βAPP, whereas APPsα continues to be secreted predominantly from the basolateral surface (24). Moreover, expressing the familial AD-associated Swedish mutation, which is known to enhance BACE-mediated βAPP processing (27, 28), reveals apical secretion of Swedish-APPsβ (21, 22).

Understanding the cellular sorting pathways associated with proteolytic processing of βAPP and, specifically, the mechanisms that allow the secretase activities to come into contact with their substrate βAPP will help reveal and prevent amyloidogenesis. We therefore analyzed the sorting of BACE and its enzymatic activity in terms of Aβ production in polarized

* This work was supported by the Deutsche Forschungsgemeinschaft (SFB 596 Molecular Mechanisms of Neurodegeneration (Project B1)) and by the Boehringer Ingelheim K.G. The costs of publication of this article were defrayed in part by the payment of page charges. This article must therefore be hereby marked "*advertisement*" in accordance with 18 U.S.C. Section 1734 solely to indicate this fact.

¶ To whom correspondence should be addressed. Tel.: 49-89-5996-471/472; Fax: 49-89-5996-415; E-mail: chaass@pbm.med.uni-muenchen.de.

[1] The abbreviations used are: Aβ, amyloid β-peptide; AD, Alzheimer's disease; βAPP, β-amyloid precursor protein; BACE, β-site APP cleaving enzyme; MDCK, Madin-Darby canine kidney; CTF, C-terminal fragment; APPsα and APPsβ, APP-soluble α cut and β cut; PBS, phosphate-buffered saline; BSA, bovine serum albumin; MES, 2-*N*-morpholinoethanesulfonic acid; wt, wild type; PS, presenilin; NHS-LC, sulfosuccinimidyl-6-(biotinamido)hexanoate.

cells. Parallel investigation of the α- and γ-secretase activity revealed differential sorting of the two amyloidogenic secretases and their substrate βAPP. This sorting mechanism apparently limits Aβ production, by allowing efficient competition of the exclusive basolateral α-secretase activity with the low amounts of basolaterally sorted BACE.

EXPERIMENTAL PROCEDURES

cDNA Constructs—cDNA constructs encoding BACE were amplified by PCR and subcloned into the *Eco*RI/*Xho*I site of the pcDNA3.1/zeo(+) expression vector (Invitrogen) as described previously (29).

Tissue Culture—MDCK cells (strain II) were maintained in Dulbecco's modified Eagle's medium supplemented with 10% fetal bovine serum and antibiotics. All stable transfections of MDCK cells were performed with FuGENE (Roche Diagnostics) as described by the manufacturer. Cell lines expressing BACE or presenilin constructs from pcDNA3.1/Zeo were selected with 400 $\mu g\ ml^{-1}$ zeocin. Cell lines with moderate expression levels and normal morphology were selected for the study. To obtain polarized monolayers for surface biotinylation or metabolic labeling, cells were plated at confluence on 24-mm polycarbonate Transwell filter (Corning Costar Corp.). For immunocytochemistry cells were plated on a 12-mm diameter filter. Media were changed each day, and cells were used for the corresponding experiment after 5–6 days. To increase expression levels cells were treated overnight with 10 mM butyrate. Similar results were obtained with untreated and treated cells.

Primary cultures of hippocampal neurons were prepared and cultured according to standard conditions.

Antibodies—The polyclonal antibodies 7523 and GM190 directed to the N terminus (amino acids 46–60) and the pro-peptide (amino acids 22–45) of BACE were described previously (29). The polyclonal antibody 3027 against the large loop of PS1 and the monoclonal antibody PS1N against the N terminus of PS1 were described previously (30).

Immunocytochemistry and Confocal Imaging—Cells grown on filters were washed with PBS containing 1 mM $CaCl_2$, 0.5 mM $MgCl_2$ (PBS^+). Antibody 7523 (1:100 in 0.2% BSA/PBS^+) was added to the apical or basolateral surface for 30 min at 4 °C. After extensive washing in PBS^+, cells were fixed in 4% paraformaldehyde/PBS^+ for 30 min at 4 °C, quenched for 10 min in 50 mM NH_4Cl/PBS^+, and then incubated with the fluorochrome-conjugated secondary antibody (Alexa 488, Molecular Probes, 1:250) for 45 min at 37 °C. After extensive washing, filters were cut out and mounted in Moviol. Confocal images were obtained with a Leica TCS SP confocal laser scanning microscope (Leica Microsystems) equipped with an oil immersion plan-apochromatic 100/1.4 numerical aperture objective lens. Fluorochromes were visualized using an argon laser with excitation wavelengths of 488 nm, emission filter 490–530 nm (for Alexa 488). Images were recorded with 512- × 512-pixel resolution and processed with Photoshop version 5.5 (Adobe Systems, Inc.). Hippocampal neurons were transfected with an endotoxin-free BACE cDNA using Effectene (Qiagen). 36 h after transfection, neurons were fixed and stained with the affinity-purified antibody 7523 and costained with a monoclonal anti-MAP-2 antibody.

Metabolic Labeling and Immunoprecipitation—For pulse-chase experiments, MDCK cells grown on Transwell filters were starved for 45 min in methionine- and serum-free minimal essential medium and subsequently metabolically labeled with 300 μCi of [^{35}S]methionine/[^{35}S]cysteine (Promix, Amersham Biosciences, Inc.) in methionine- and serum-free minimal essential medium for 10 min and chased in the presence of excess amounts of unlabeled methionine for the indicated time points. Cells were lysed in buffer containing 1% Nonidet P-40 on ice for 30 min and scraped from the filter, and lysates were clarified by centrifugation for 20 min at 14,000 × *g*. Immunoprecipitation and separation by SDS-PAGE was performed as described previously (29). For the immunoprecipitation of APPs and Aβ, cells were metabolically labeled for 4 h using 300 μCi of Promix in methionine-free media containing 5% dialyzed serum. Media collected from the apical and basolateral chamber were immunoprecipitated. Quantitation was performed by phosphorimaging (PhosphorImager, Molecular Dynamics).

Surface Biotinylation—MDCK cells were grown on filters for 5 days. The monolayer was washed three times with cold PBS^+, followed by incubation with sulfo-NHS-LC-biotin (1 mg/ml, Pierce) either apically or basolaterally for 1 h at 4 °C. 1% BSA in PBS^+ was added to the opposite chamber. The reaction was stopped by washing with PBS^+ and quenched with 10 mM glycine, 1% BSA in PBS^+. Cell lysates were prepared and precipitated with streptavidin-Sepharose (Amersham Biosciences, Inc.). The precipitated, biotinylated proteins were separated on SDS gels and transferred to polyvinylidene difluoride membranes. For detection of BACE, PS1, or βAPP, the indicated antibody was used. Specifically bound antibodies were visualized by a horseradish peroxidase-conjugated secondary antibody using the enhanced chemiluminescence technique (Amersham Biosciences, Inc.) or an ^{125}I-conjugated secondary antibody.

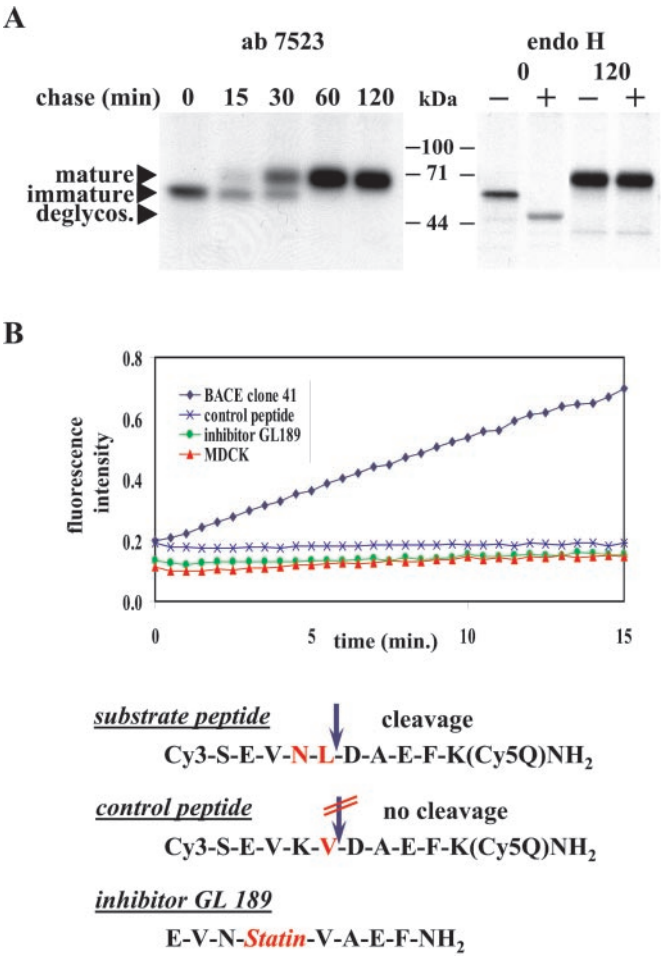

FIG. 1. **Expression and maturation of functionally active BACE in MDCK cells.** *A*, maturation of BACE in MDCK cells. *Left panel*, MDCK cells stably expressing BACE were pulse-labeled with [^{35}S]methionine/cysteine and chased for the indicated time points in the presence of excess amounts of unlabeled methionine. Cell lysates were immunoprecipitated with antibody 7523. Note that antibody 7523 preferentially detects mature BACE (29). *Right panel*, *N*-glycosylation and oligosaccharide modification of BACE. MDCK cells stably expressing BACE were pulse-labeled with [^{35}S]methionine and chased in the presence of excess amounts of unlabeled methionine for 2 h. Cell lysates were immunoprecipitated with antibody 7523 and treated with (+) and without (−) endoglycosidase H. Note that the mature form of BACE is endoglycosidase H-resistant. *B*, membranes from BACE-transfected (♦) or untransfected MDCK cells (▲) were solubilized and analyzed *in vitro* for proteolytic activity. Incubation of the fluorogenic peptide containing the Swedish mutation with solubilized membrane fractions from BACE-transfected (♦) MDCK cells allowed a significant time-dependent proteolytic reaction, whereas the non-cleavable substrate peptide with the Met to Val mutation at the P1 side is not proteolyzed (*X*). Moreover, incubation with the BACE-specific inhibitor GL189 (5 μM) blocked the proteolytic activity of solubilized membrane fractions from BACE-transfected cells (●). Untransfected MDCK cells show very little BACE activity (▲), which appears to be below the detection limit of the *in vitro* assay. Substrate peptides and the BACE-specific inhibitor GL189 are shown below. The NL mutation (Swedish mutant substrate) as well as the V mutation (non-cleavable control substrate) are shown in *red*.

Enzymatic Deglycosylation—These experiments were done as described previously (29).

Fluorometric BACE Activity Assay—A quenched fluorescence substrate Cy3-SEV**NL**DAEFK(Cy5Q)-NH_2 containing the Swedish βAPP mutation (in boldface) and a non-cleavable substrate Cy3-SEV**K**V**V**DAEFK(Cy5Q)-NH_2, containing an amino acid exchange, M →

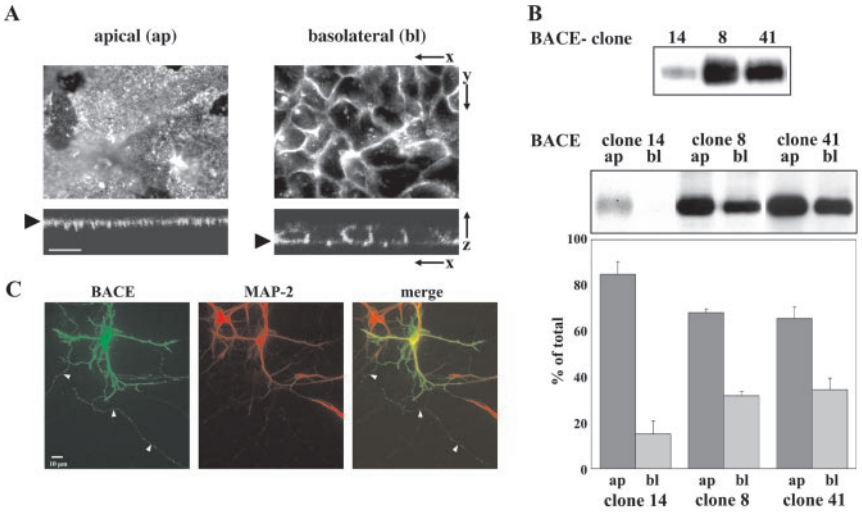

FIG. 2. **Sorting of BACE in polarized MDCK cells and rat hippocampal neurons.** *A*, immunocytochemical detection of BACE. Monolayers of MDCK cells stably expressing BACE were incubated with antibody 7523 on the basolateral or apical side. Bound antibodies were detected with a secondary fluorescent antibody. Note the detection of BACE on either side of the monolayer. *Lower panel*, vertical cross-sections (*z* axis). Basolateral and apical BACE are indicated by the *arrowheads*. *Bar*, 10 μM. *B*, expression and cell surface distribution of BACE. Three independent cell lines expressing low or high levels of BACE were analyzed (detected by immunoblotting with antibody 7523; *upper panel*). *Lower panel*, cell surface biotinylation of BACE. Biotinylated surface proteins were isolated using streptavidin-coated Sepharose. Surface-biotinylated BACE molecules were detected by immunoblotting using antibody 7523 and quantitated. Data shown are average ± S.D. of three independent experiments. *C*, axonal targeting of BACE in hippocampal neurons. 36 h after transfection of fully differentiated neurons with the human BACE cDNAs, neurons were fixed, permeabilized, and costained with the affinity-purified antibody 7523 (*BACE*) and a monoclonal anti-MAP-2 antibody (*MAP-2*) to label the somato-dendritic compartment. The merged image (*merge*) demonstrates axonal (*white arrowheads*) and somato-dendritic sorting of human BACE.

V (in boldface) were synthesized by Amersham Biosciences, Inc., UK. Membranes from BACE-transfected and non-transfected MDCK cells were prepared and extracted with 1% Triton X-100, 20 mM MES, pH 6.0, including a protease inhibitor mix (Sigma Chemical Co.). The assay was carried out in a volume of 200 μl containing 400 nM peptide substrate or the non-cleavable control peptide, 2 μl of the membrane preparation, and 20 mM sodium acetate, pH 4.4. Fluorescence was measured continuously over a period of 15 min, at room temperature (Fluoroskan Ascent, Labsystems, Finland, excitation 530 nm, emission 590 nm). The β-secretase inhibitor (GL189) H-EVNstatineVAEF-NH_2 was synthesized by K. Maskos and W. Bode.

Radiosequencing—Aβ peptides were radiosequenced as described previously (31).

RESULTS

Maturation and Enzymatic Activity of BACE in MDCK Cells—BACE mediates the initial amyloidogenic cleavage, which produces the direct precursor for Aβ production. Due to the pivotal importance of this cleavage, we first investigated BACE maturation and its proteolytic activity in MDCK cells. Because endogenous levels of BACE are too low to allow its direct biochemical and cellular analysis (2), we stably transfected MDCK cells as well as a previously described MDCK cell line (23) overexpressing human wt βAPP with a BACE cDNA expression construct. In addition to overexpressed BACE, we also monitored the distribution of endogenous BACE activity by analyzing its primary cleavage product APPsβ (see below). MDCK cells stably expressing human BACE were analyzed in pulse-chase experiments for maturation and glycosylation of BACE. After a short pulse, immature BACE is detected by immunoprecipitation of cell lysates with antibody 7523 (29) (Fig. 1*A*). Over time, efficient maturation to a higher molecular weight variant was observed (Fig. 1*A*), which lacks the propeptide (data not shown). The fully glycosylated high molecular weight BACE variant reaches a post-Golgi compartment as demonstrated by the selective resistance of this variant against endoglycosidase H (Fig. 1*A*). We next investigated whether overexpressed BACE is catalytically active in MDCK cells. Membranes were prepared from BACE-transfected and untransfected MDCK cell lines. Solubilized membrane fractions were incubated with a fluorogenic βAPP-derived peptide extending from P5 to P5′ containing the Swedish mutation (Fig. 1*B*). This peptide contains one of the two known cleavage sites of BACE (see below). Compared with membrane extracts from untransfected cells, a high proteolytic activity is present in extracts derived from a BACE-transfected cell line (Fig. 1*B*). When solubilized membranes of BACE-transfected cells were incubated with the BACE inhibitor GL189 (Fig. 1*B*), a complete inhibition of the proteolytic activity was observed (Fig. 1*B*). Finally, we used a peptide, which contained a Met to Val substitution at the P1 site (Fig. 1*B*). This mutation was previously shown to inhibit endoproteolytic cleavage by BACE (2, 32). Consistent with these observations, the mutant peptide was not proteolyzed in the *in vitro* assay containing solubilized membrane fractions from BACE-transfected cells (Fig. 1*B*). These results thus demonstrate that fully mature biologically active BACE with its expected biochemical features is expressed in MDCK cells. In addition to the cleavage at the critical Asp-1 of the Aβ domain, we also detected significant cleavage activity at Glu-11 (see below), which is consistent with previous reports (2, 33–36) and represents another major *in vivo* cleavage site of BACE.

Surface Distribution of BACE—To determine the surface distribution of BACE, the MDCK cell lines described above were grown on Transwell filters to form polarized monolayers. These were incubated with antibody 7523 to the ectodomain of BACE on the apical or basolateral surface. Laser confocal microscopy revealed BACE expression on each surface (Fig. 2*A*). This was further confirmed by analyzing vertical cross-section (*z* axis) of polarized monolayers (Fig. 2*A*, *lower panel*).

Cell surface targeting of BACE was analyzed by direct biotinylation of mature BACE at the plasma membrane. Three individual MDCK cell lines, which express different levels of BACE, were selected (Fig. 2*B*). In addition to two high expressing lines (*lines 8* and *41*) a low expressing line (*line 14*) was chosen to avoid saturation of polarized sorting. Polarized monolayers were chilled to 4 °C and labeled with sulfo-NHS-LC-biotin on the basolateral or the apical side. After lysis, biotiny-

lated surface proteins were isolated using streptavidin-coated Sepharose. Surface-biotinylated BACE molecules were detected by immunoblotting using antibody 7523. This revealed that the mature BACE variant is exclusively targeted to both cell surfaces (Fig. 2*B*). No pro-peptide-containing immature BACE was detected on the cell surface (data not shown). Quantitation of multiple experiments with three independent individual cell lines revealed that ~70–80% of BACE are targeted to the apical surface, whereas only about 20–30% were found on the basolateral surface (Fig. 2*B*) where most of the βAPP substrate is located (23). The low expressing line showed the most efficient apical targeting of BACE (Fig. 2*B*) indicating that apical sorting of BACE can be affected by very high expression levels.

The sorting of BACE to the apical compartment together with about 20–30% basolateral targeting suggests that BACE is expressed in neurons in axons as well as in the somato-dendritic compartment (20). To prove this, fully differentiated rat hippocampal neurons were transfected with a BACE cDNA. Cells were costained with antibody 7523 to BACE and with an anti-MAP2 antibody to specifically identify somato-dendritic compartments. As shown in Fig. 2*C*, BACE is indeed targeted to both axons and somato-dendritic compartments.

Basolaterally Sorted BACE and α-Secretase Compete for βAPP—We next investigated the polarized distribution of α- and β-secretase products in MDCK cell lines, which overexpress either human βAPP alone or together with BACE. Aliquots of conditioned media from metabolically labeled cells were immunoprecipitated with the neo-epitope-specific antibody 1736 (Fig. 3*A*) (37), which specifically detects α-secretase-generated soluble APPsα. As reported previously (24), cells expressing only βAPP secreted APPsα basolaterally (Fig. 3*B*). In contrast, the additional expression of BACE resulted in very low levels of APPsα secretion (Fig. 3*B*). In fact, basolateral secretion of APPsα was selectively reduced (Fig. 3*B*). This suggests that overexpressed BACE is competing with endogenous α-secretase within the basolateral targeting pathway, thus producing APPsβ (which is not detected by antibody 1736) to the expense of APPsα.

To determine the amounts of APPsβ produced by BACE, we immunoprecipitated secreted APPs species with antibody 5313 (38), which allows detection of both APPsα and APPsβ (Fig. 3*A*), and compared the immunoprecipitated species with APPsα isolated with antibody 1736 (Fig. 3*A*). In clear contrast to antibody 1736 (Fig. 3*B*), antibody 5313 detected robust levels of secreted APPs in both compartments of MDCK cells overexpressing BACE and βAPP (Fig. 3*C*). These migrated to a slightly lower molecular weight consistent with BACE-generated truncated APPsβ (27, 28). Moreover, quantitation (by calculating the difference between total APPs precipitated by antibody 5313 and APPsα isolated by antibody 1736) revealed equal secretion of APPsβ into the apical and basolateral compartments of double-transfected cells (Fig. 3*D*). This result demonstrates that APPsβ can be secreted at both surfaces (Fig. 3, *C* and *D*), whereas APPsα is almost exclusively secreted from the basolateral side (Fig. 3*B*). This is supported by the finding that APPsβ is also secreted into the apical and basolateral compartment by cells not transfected with BACE (Fig. 3, *C* and *D*). However, the significant increase of total APPsβ secretion into the basolateral and apical compartments upon BACE overexpression indicates cleavage of βAPP before it reaches the sorting compartment within the *trans*-Golgi (see "Discussion").

Apically Missorted βAPP Is Efficiently Proteolyzed by BACE and γ-Secretase—The above described results suggest a high endogenous BACE activity on the apical side, where it can produce APPsβ in equal amounts as on the basolateral side,

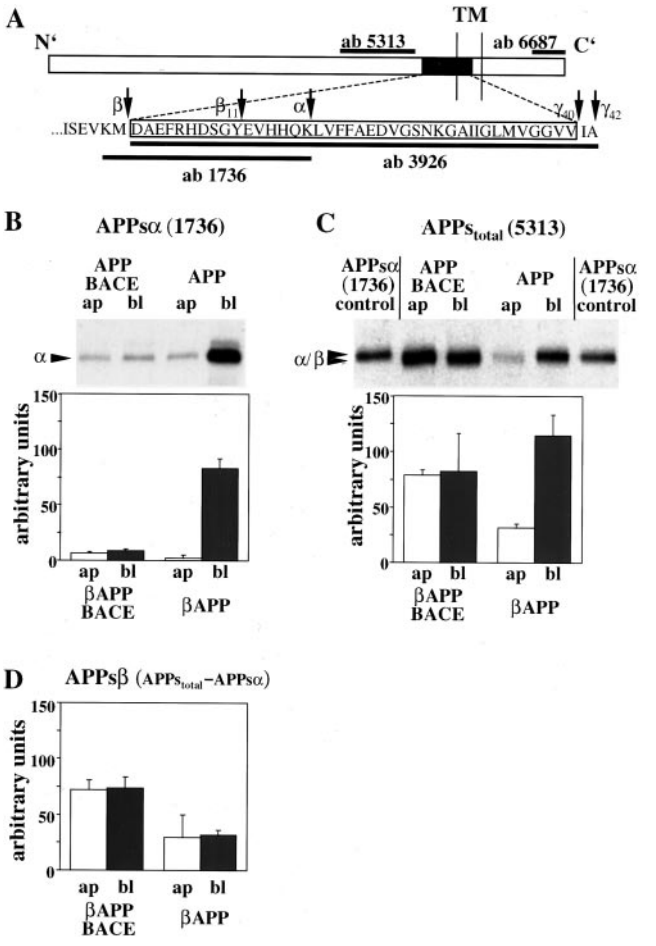

FIG. 3. **Polarized secretion of APPsα and APPsβ.** *A*, schematic representation of βAPP. The sites of secretase cleavages (*arrows*) and epitopes used for immunization (*bars*) are indicated. *B*, polarized secretion of APPsα. Conditioned media of MDCK cells stably transfected with βAPP and BACE, or βAPP alone were immunoprecipitated with antibody 1736 to exclusively identify APPsα. *Lower panel*, quantitation of the amounts of APPsα secreted on either side of the polarized monolayer. Data shown are average ± S.D. of three independent experiments. *C*, polarized secretion of total APPs (APPsα and APPsβ). Conditioned media of MDCK cells transfected with βAPP and BACE, or βAPP alone were immunoprecipitated with antibody 5313 to identify APPsα and APPsβ. Antibody 5313 detects higher levels of APPs within the basolateral than in the apical compartment of cells expressing only βAPP. This is due to the fact that these cells also secrete high levels of APPsα (compare immunoprecipitations with antibody 1736 in *B*). *Lower panel*, quantitation of the amounts of total APPs secreted on either side of the polarized monolayer. Data shown are average ± S.D. of three independent experiments. *D*, quantitation of the amounts of APPsβ secreted on either side of the polarized monolayer. The amounts of APPsβ were determined by calculating the difference of total APPs and APPsα. Data shown are average ± S.D. of three independent experiments. Note that both antibodies have similar affinities to APPs (data not shown).

although only about 10% of the βAPP holoprotein is targeted to the apical side. This indicates a very efficient BACE-mediated processing of apically sorted βAPP probably due to the lack of apical α-secretase activity. To prove this, we expressed a C-terminally truncated βAPP derivative (βAPPΔC), which we have shown previously to be targeted to both surfaces due to the loss of the cytoplasmic sorting signal (24). Aliquots of conditioned media from metabolically labeled MDCK cells expressing βAPPΔC were immunoprecipitated with neo-epitope-specific antibody 1736 or with antibody 5313. As shown before (24), APPsα is almost exclusively secreted into the basolateral compartment, independently of the sorting of the βAPP holoprotein (Fig. 4). In contrast, a significant increase of APPsβ secretion

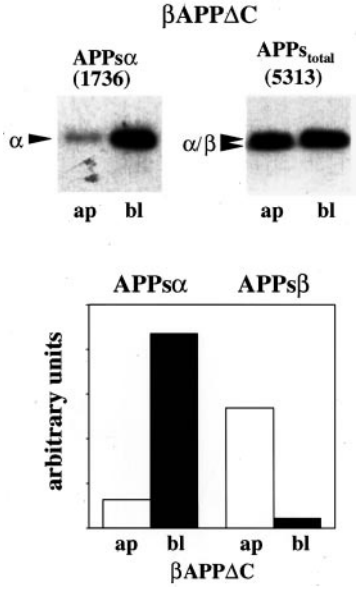

FIG. 4. **Missorting of βAPP differentially affects processing by α- and β-secretase.** MDCK cells overexpressing βAPPΔC were metabolically labeled and conditioned media were immunoprecipitated with antibody 1736 or antibody 5313. APPsα and APPsβ secretion was quantitated as described above.

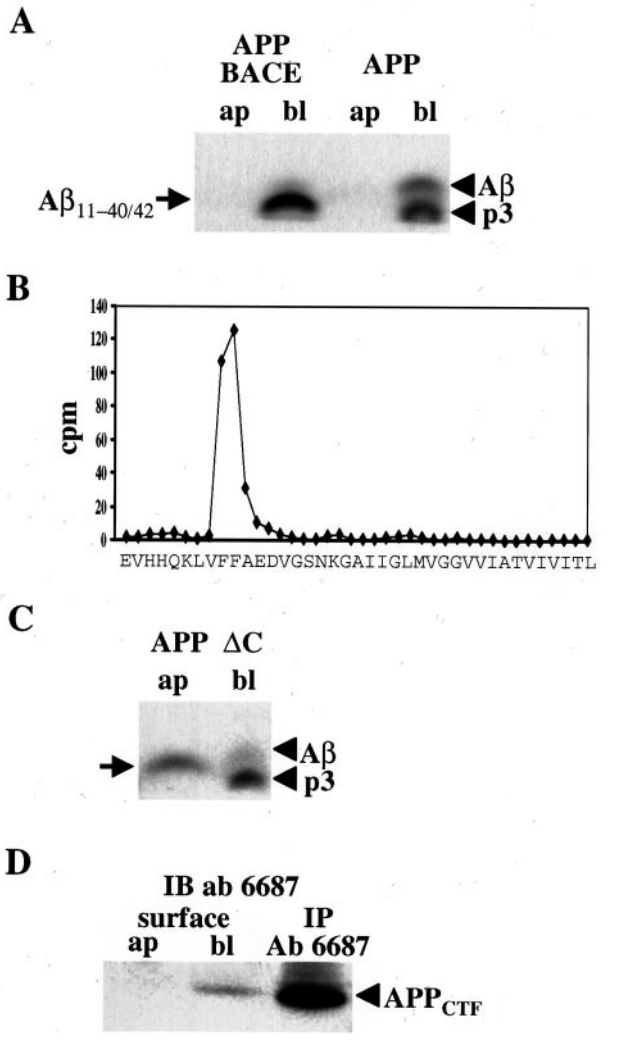

FIG. 5. **Apical BACE and γ-secretase activity.** *A*, polarized distribution of Aβ and p3 in cells expressing βAPP alone or βAPP and BACE. Conditioned media was immunoprecipitated with antibody 3926 (39). Note the enhanced production of a truncated Aβ species in cells double-transfected with βAPP and BACE (*arrow*). *B*, radiosequencing of Aβ secreted from BACE-expressing cells. Cells were metabolically labeled with [^{3}H]Phe, and Aβ was isolated from conditioned media by immunoprecipitation with antibody 3926. The peak of radioactivity in cycles 9 and 10 demonstrates that the N terminus of this Aβ species begins at Glu-11. *C*, polarized distribution of Aβ and p3 in cells expressing βAPPΔC. Conditioned media were immunoprecipitated with antibody 3926. Note that Aβ peptides are secreted on both sides, whereas p3 is exclusively observed within the basolateral compartment. Consistent with previous findings, increased levels of p3 are found upon deletion of the βAPP cytoplasmic domain (24). A truncated Aβ species (most likely starting at Glu-11; see above) is found predominantly on the apical side (*arrow*). *D*, detection of βAPP CTFs on the basolateral cell surface. Biotinylated surface proteins were isolated using streptavidin-coated Sepharose. Surface-biotinylated βAPP CTFs were detected by immunoblotting using antibody 6687. As shown by the direct immunoprecipitation with antibody 6687, the α-secretase-generated βAPP CTF is very abundant in MDCK cells, whereas only very small amounts of β-secretase generated βAPP CTFs where observed.

into the apical compartment is observed (Fig. 4). Therefore, apically sorted full-length βAPP is almost exclusively cleaved by BACE, whereas basolateral βAPP appears to be processed by α- and β-secretase in a competitive manner. It is important to note that the distribution of endogenous BACE activity in the presence of mistargeted βAPP reflects the distribution of cell-surface biotinylated BACE (compare Fig. 4 with Fig. 2) thus indicating apical sorting of endogenous BACE similar to that of overexpressed BACE. To further prove this, we next compared polarized Aβ and p3 secretion in MDCK cells overexpressing βAPP/BACE or βAPP alone. Conditioned media from the apical and basolateral compartment were immunoprecipitated with antibody 3926 (39) (Fig. 5*A*). In cells expressing βAPP alone, Aβ and p3 were almost exclusively secreted into the basolateral compartment (Fig. 5*A*). In cells expressing both βAPP and BACE, no p3 was detected (Fig. 5*A*), consistent with the competitive reduction of α-secretory processing, described above (Fig. 3*B*). Instead, high levels of an Aβ species migrating between native Aβ and p3 were observed in the double-transfected cells (Fig. 5*A*). Radiosequencing of this peptide revealed that its N terminus begins predominantly at Glu-11 (Fig. 5*B*). Cleavage at Glu-11 is a typical feature of the β-secretase activity and is observed in cells expressing endogenous (see below) (31) and overexpressed BACE (2, 33–36). The truncated Aβ species is secreted only basolaterally, although the corresponding APPsβ is equally secreted into the apical and basolateral compartment (see Fig. 3*D*). The reason might be that the precursor of Aβ, the BACE-generated βAPP CTF, still contains the sorting signal for basolateral transport (see Fig. 5*D* for further evidence). We next investigated if a similar truncated Aβ species could be produced on the apical side, where high levels of BACE, but little, if any, α-secretase activity was observed. To do so, βAPPΔC was expressed, which allows the trafficking of significant amounts of the βAPP holoprotein to the apical side (24). In contrast to the basolateral secretion of Aβ/p3 in wt βAPP-expressing cells, overexpression of the C-terminally truncated βAPP derivative revealed Aβ secretion from both surfaces (Fig. 5*C*). Indeed, high levels of a truncated Aβ species were observed on the apical side. Due to the preferentially apical distribution of BACE and the competition of BACE with α-secretase on the opposite side, smaller amounts of Aβ were detected basolaterally (Fig. 5*C*). Moreover, consistent with the above described basolateral activity of α-secretase (Figs. 3*B* and 4) p3 was exclusively observed in the basolateral compartment (Fig. 5*C*). Efficient Aβ production on the apical site again supports the notion that endogenous BACE undergoes predominantly apical targeting like the overexpressed enzyme. This also demonstrates that the Glu-11

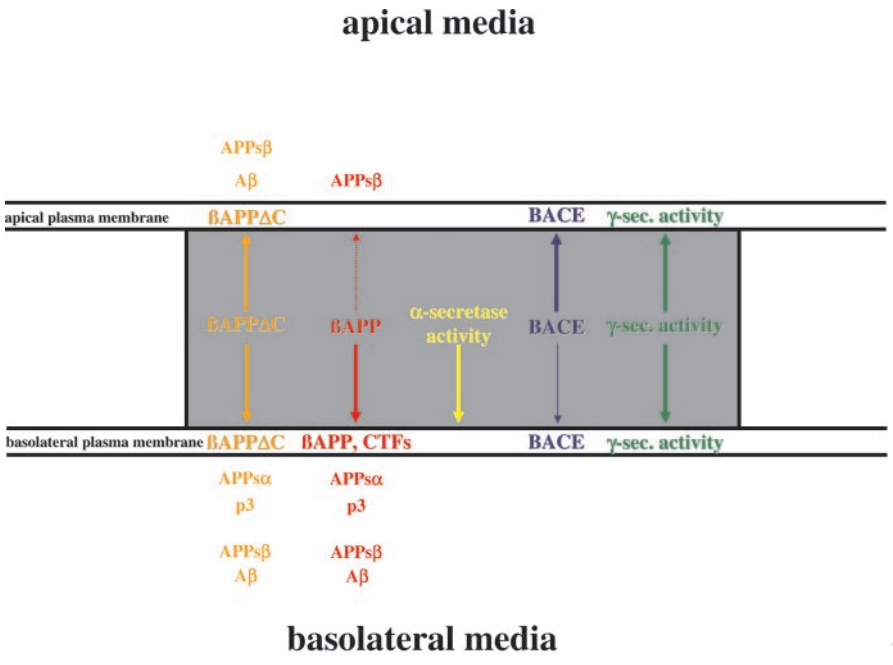

FIG. 6. **Schematic representation of the polarized sorting of βAPP, the secretase activities, and their cleavage products.** For details, see "Discussion."

cleavage can also be observed in the absence of BACE overexpression. Moreover, it also demonstrates that significant levels of γ-secretase activity must undergo apical sorting.

The exclusive basolateral secretion of Aβ in cells expressing the wild type βAPP holoprotein might be due to a basolateral sorting of the immediate γ-secretase substrates and may thus not necessarily reflect the distribution of the γ-secretase activity. If that is the case, the βAPP CTFs generated by β- and α-secretase (which are the substrate for γ-secretase) should be observed on the basolateral plasma membrane, because these fragments still contain the required targeting information within their cytoplasmic tails (24). We therefore investigated the distribution of such fragments in MDCK cells overexpressing βAPP alone. Surface-biotinylated βAPP fragments were precipitated with streptavidin beads and detected by immunoblotting using antibody 6687 (38). This indeed revealed the presence of βAPP CTFs predominantly on the basolateral surface (Fig. 5*D*), thus demonstrating a highly polarized distribution of these immediate precursors for amyloidogenesis.

From these results we conclude that amyloidogenic processing of βAPP by BACE is determined by the differential distribution of the β-secretase activity and its substrate βAPP. Due to the lower levels of basolateral BACE and the competition of BACE and α-secretase for basolaterally sorted βAPP, Aβ production is limited. Moreover, in contrast to the basolateral sorting of βAPP, γ-secretase activity is also efficiently sorted to the apical side.

DISCUSSION

Based on the results described above the following picture of polarized βAPP processing and its interaction with the secretase activities is emerging (Fig. 6). Membrane-bound full-length βAPP is targeted predominantly to the basolateral cell surface. In contrast to its substrate, BACE is sorted preferentially to the apical surface. This is observed upon overexpression, however, endogenous BACE activity also undergoes similar sorting. The α- and β-secretase-generated βAPP CTFs, which are the immediate precursors for the γ-secretase cleavage to produce Aβ and p3 (1), are targeted to the basolateral membrane, because they contain their cytoplasmic basolateral sorting signal. At the basolateral membrane or close to it the final γ-secretase cleavage takes place, which liberates either Aβ or p3 (Fig. 6). In contrast, γ-secretase activity is sorted to both cell surfaces. Consequently, βAPP can be a substrate for γ-secretase at or close to both surfaces. This does not necessarily imply that PSs are also targeted to both surfaces, because PSs do not overlap with βAPP in late secretory compartments, a phenomenon described as the spatial paradox (40). α-Secretase activity is located on the basolateral side, because its products p3 as well as APPsα are both almost exclusively detected within the basolateral compartment (Fig. 6). Thus α- and β-secretase can compete for their substrates only on the basolateral sorting pathway, a cellular mechanism that apparently determines the levels of Aβ generation in polarized cells.

Basolateral sorting of α-secretase activity explains the previous paradoxical finding on the sorting of βAPP upon the deletion of its cytoplasmic sorting signal. Under these conditions the holoprotein is targeted to both surfaces, although APPsα continues to be secreted basolateral (24). Our findings demonstrate that this is due to the predominantly basolateral activity of α-secretase, which consequently supports preferential basolateral secretion of APPsα and p3 even if half of the βAPP molecules are mistargeted to the apical surface.

In contrast to APPsα, APPsβ is secreted from both surfaces in almost equal amounts. However, as described above only small amounts of βAPP reach the apical surface, whereas the majority is targeted to the basolateral side. The equal amounts of secreted APPsβ on the apical and basolateral side of MDCK cells expressing endogenous BACE are due to cellular mechanisms, which support BACE-mediated cleavage on the way to the apical surface but reduce BACE-mediated cleavage on the basolateral side. First, on the way to the basolateral side βAPP is cleaved by the competing α-secretases, which consequently reduces the amounts of βAPP available for BACE cleavage. Second, because α-secretory activity was only observed on the basolateral side, the rather small amounts of βAPP, which are targeted to the apical side, are an almost exclusive substrate for BACE. Upon overexpression of BACE, very efficient β-secretory processing is observed at the expense of α-secretory processing. Under these conditions BACE appears to cleave before α-secretase. Thus it is likely that overexpressed BACE has cleaved βAPP already before it reaches the *trans*-Golgi network, the compartment known to be required for polarized

sorting in MDCK cells (41, 42). Consequently, the strongly increased APPsβ undergoes unpolarized secretion. In contrast, the membrane-bound cleavage products of BACE, the βAPP CTFs, which are the immediate precursors for Aβ generation, still contain their cytoplasmic sorting signal and are consequently targeted to the basolateral side where they can be further processed to Aβ (see above).

Finally, our data suggest that, at least in MDCK cells, βAPP is not the major physiological substrate of BACE, because both are targeted in the opposite direction. This is supported by the observation that the β-secretase activity in mice is unable to efficiently cleave endogenous βAPP whereas human βAPP, which has a slightly different amino acid sequence in its Aβ domain, is cleaved normally (43). Therefore, βAPP cannot be the major BACE substrate in mice as well. Indeed, while this report was under review, a novel BACE substrate was identified (44).

Acknowledgments—We thank Dennis Selkoe for antibody 1736; Gerd Multhaup for antibody GM190; Inga Maertens for technical support; Klaus Maskos and Wolfram Bode for the generation of GL189; Christoph Kaether, Harald Steiner, and Philipp Kahle for critical discussion; and Olga Alexandrova for the help with confocal microscopy.

REFERENCES

1. Steiner, H., and Haass, C. (2000) *Nat. Rev. Mol. Cell Biol.* **1,** 217–224
2. Vassar, R., Bennett, B. D., Babu-Khan, S., Kahn, S., Mendiaz, E. A., Denis, P., Teplow, D. B., Ross, S., Amarante, P., Loeloff, R., Luo, Y., Fisher, S., Fuller, J., Edenson, S., Lile, J., Jarosinski, M. A., Biere, A. L., Curran, E., Burgess, T., Louis, J. C., Collins, F., Treanor, J., Rogers, G., and Citron, M. (1999) *Science* **286,** 735–741
3. Yan, R., Bienkowski, M. J., Shuck, M. E., Miao, H., Tory, M. C., Pauley, A. M., Brashier, J. R., Stratman, N. C., Mathews, W. R., Buhl, A. E., Carter, D. B., Tomasselli, A. G., Parodi, L. A., Heinrikson, R. L., and Gurney, M. E. (1999) *Nature* **402,** 533–537
4. Lin, X., Koelsch, G., Wu, S., Downs, D., Dashti, A., and Tang, J. (2000) *Proc. Natl. Acad. Sci. U. S. A.* **97,** 1456–1460
5. Sinha, S., Anderson, J. P., Barbour, R., Basi, G. S., Caccavello, R., Davis, D., Doan, M., Dovey, H. F., Frigon, N., Hong, J., Jacobson-Croak, K., Jewett, N., Keim, P., Knops, J., Lieberburg, I., Power, M., Tan, H., Tatsuno, G., Tung, J., Schenk, D., Seubert, P., Suomensaari, S. M., Wang, S., Walker, D., Zhao, J., McConlogue, L., and John, V. (1999) *Nature* **402,** 537–540
6. Hussain, I., Powell, D., Howlett, D. R., Tew, D. G., Meek, T. D., Chapman, C., Gloger, I. S., Murphy, K. E., Southan, C. D., Ryan, D. M., Smith, T. S., Simmons, D. L., Walsh, F. S., Dingwall, C., and Christie, G. (1999) *Mol. Cell. Neurosci.* **14,** 419–427
7. Seubert, P., Oltersdorf, T., Lee, M. G., Barbour, R., Blomquist, C., Davis, D. L., Bryant, K., Fritz, L. C., Galasko, D., Thal, L. J., Lieberburg, I., and Schenk, D. (1993) *Nature* **361,** 260–263
8. Herreman, A., Serneels, L., Annaert, W., Collen, D., Schoonjans, L., and De Strooper, B. (2000) *Nat. Cell Biol.* **2,** 461–462
9. De Strooper, B., Saftig, P., Craessaerts, K., Vanderstichele, H., Guhde, G., Annaert, W., Von Figura, K., and Van Leuven, F. (1998) *Nature* **391,** 387–390
10. Zhang, Z., Nadeau, P., Song, W., Donoviel, D., Yuan, M., Bernstein, A., and Yankner, B. A. (2000) *Nat. Cell Biol.* **2,** 463–465
11. Wolfe, M. S., De Los Angeles, J., Miller, D. D., Xia, W., and Selkoe, D. J. (1999) *Biochemistry* **38,** 11223–11230
12. Wolfe, M. S., Xia, W., Ostaszewski, B. L., Diehl, T. S., Kimberly, W. T., and Selkoe, D. J. (1999) *Nature* **398,** 513–517
13. Esler, W. P., Kimberly, W. T., Ostaszewski, B. L., Diehl, T. S., Moore, C. L., Tsai, J.-Y., Rahmati, T., Xia, W., Selkoe, D. J., and Wolfe, M. S. (2000) *Nat. Cell Biol.* **2,** 428–433
14. Li, Y.-M., Xu, M., Lai, M.-T., Huang, Q., Castro, J. L., DiMuzio-Mower, J., Harrison, T., Lellis, C., Nadin, A., Neduvelli, J. G., Register, R. B., Sardana, M. K., Shearman, M. S., Smith, A. L., Shi, X.-P., Yin, K.-C., Shafer, J. A., and Gardell, S. J. (2000) *Nature* **405,** 689–694
15. Steiner, H., Kostka, M., Romig, H., Basset, G., Pesold, B., Hardy, J., Capell, A., Meyn, L., Grim, M. G., Baumeister, R., Fechteler, K., and Haass, C. (2000) *Nat. Cell Biol.* **2,** 848–851
16. Sastre, M., Steiner, H., Fuchs, K., Capell, A., Multhaup, G., Condron, M. M., Teplow, D. B., and Haass, C. (2001) *EMBO Rep.* **2,** 835–841
17. Koike, H., Tomioka, S., Sorimachi, H., Saido, T. C., Maruyama, K., Okuyama, A., Fujisawa-Sehara, A., Ohno, S., Suzuki, K., and Ishiura, S. (1999) *Biochem. J.* **343,** 371–375
18. Lammich, S., Kojro, E., Postina, R., Gilbert, S., Pfeiffer, R., Jasionowski, M., Haass, C., and Fahrenholz, F. (1999) *Proc. Natl. Acad. Sci. U. S. A.* **96,** 3922–3927
19. Buxbaum, J. D., Liu, K. N., Luo, Y., Slack, J. L., Stocking, K. L., Peschon, J. J., Johnson, R. S., Castner, B. J., Cerretti, D. P., and Black, R. A. (1998) *J. Biol. Chem.* **273,** 27765–27767
20. Dotti, C. G., and Simons, K. (1990) *Cell* **62,** 63–72
21. Lo, A. C., Haass, C., Wagner, S. L., Teplow, D. B., and Sisodia, S. S. (1994) *J. Biol. Chem.* **269,** 30966–30973
22. De Strooper, B., Craessaerts, K., Dewachter, I., Moechars, D., Greenberg, B., Van Leuven, F., and Van den Berghe, H. (1995) *J. Biol. Chem.* **270,** 4058–4065
23. Haass, C., Koo, E. H., Teplow, D. B., and Selkoe, D. J. (1994) *Proc. Natl. Acad. Sci. U. S. A.* **91,** 1564–1568
24. Haass, C., Koo, E. H., Capell, A., Teplow, D. B., and Selkoe, D. J. (1995) *J. Cell Biol.* **128,** 537–547
25. Tienari, P. J., De Strooper, B., Ikonen, E., Simons, M., Weidemann, A., Czech, C., Hartmann, T., Ida, N., Multhaup, G., Masters, C. L., Van Leuven, F., Beyreuther, K., and Dotti, C. G. (1996) *EMBO J.* **15,** 5218–5229
26. Yamazaki, T., Selkoe, D. J., and Koo, E. H. (1995) *J. Cell Biol.* **129,** 431–442
27. Haass, C., Lemere, C. A., Capell, A., Citron, M., Seubert, P., Schenk, D., Lannfelt, L., and Selkoe, D. J. (1995) *Nat. Med.* **1,** 1291–1296
28. Thinakaran, G., Teplow, D. B., Siman, R., Greenberg, B., and Sisodia, S. S. (1996) *J. Biol. Chem.* **271,** 9390–9397
29. Capell, A., Steiner, H., Willem, M., Kaiser, H., Meyer, C., Walter, J., Lammich, S., Multhaup, G., and Haass, C. (2000) *J. Biol. Chem.* **275,** 30849–30854
30. Walter, J., Grunberg, J., Capell, A., Pesold, B., Schindzielorz, A., Citron, M., Mendla, K., George-Hyslop, P. S., Multhaup, G., Selkoe, D. J., and Haass, C. (1997) *Proc. Natl. Acad. Sci. U. S. A.* **94,** 5349–5354
31. Haass, C., Schlossmacher, M. G., Hung, A. Y., Vigo-Pelfrey, C., Mellon, A., Ostaszewski, B. L., Lieberburg, I., Koo, E. H., Schenk, D., Teplow, D. B., and Selkoe, D. J. (1992) *Nature* **359,** 322–325
32. Citron, M., Teplow, D. B., and Selkoe, D. J. (1995) *Neuron* **14,** 661–670
33. Creemers, J. W., Ines Dominguez, D., Plets, E., Serneels, L., Taylor, N. A., Multhaup, G., Craessaerts, K., Annaert, W., and De Strooper, B. (2001) *J. Biol. Chem.* **276,** 4211–4217
34. Farzan, M., Schnitzler, C. E., Vasilieva, N., Leung, D., and Choe, H. (2000) *Proc. Natl. Acad. Sci. U. S. A.* **97,** 9712–9717
35. Cai, H., Wang, Y., McCarthy, D., Wen, H., Borchelt, D. R., Price, D. L., and Wong, P. C. (2001) *Nat. Neurosci.* **4,** 233–234
36. Benjannet, S., Elagoz, A., Wickham, L., Mamarbachi, M., Munzer, J. S., Basak, A., Lazure, C., Cromlish, J. A., Sisodia, S., Checler, F., Chretien, M., and Seidah, N. G. (2001) *J. Biol. Chem.* **276,** 10879–10887
37. Haass, C., Hung, A. Y., and Selkoe, D. J. (1991) *J. Neurosci.* **11,** 3783–3793
38. Steiner, H., Duff, K., Capell, A., Romig, H., Grim, M. G., Lincoln, S., Hardy, J., Yu, X., Picciano, M., Fechteler, K., Citron, M., Kopan, R., Pesold, B., Keck, S., Baader, M., Tomita, T., Iwatsubo, T., Baumeister, R., and Haass, C. (1999) *J. Biol. Chem.* **274,** 28669–28673
39. Wild-Bode, C., Yamazaki, T., Capell, A., Leimer, U., Steiner, H., Ihara, Y., and Haass, C. (1997) *J. Biol. Chem.* **272,** 16085–16088
40. Annaert, W. G., Levesque, L., Craessaerts, K., Dierinck, I., Snellings, G., Westaway, D., George-Hyslop, P. S., Cordell, B., Fraser, P., and De Strooper, B. (1999) *J. Cell Biol.* **147,** 277–294
41. Matter, K., and Mellman, I. (1994) *Curr. Opin. Cell Biol.* **6,** 545–554
42. Keller, P., and Simons, K. (1997) *J. Cell Sci.* **110,** 3001–3009
43. De Strooper, B., Simons, M., Multhaup, G., Van Leuven, F., Beyreuther, K., and Dotti, C. G. (1995) *EMBO J.* **14,** 4932–4938
44. Kitazume, S., Tachida, Y., Oka, R., Shirotani, K., Saido, T. C., and Hashimoto, Y. (2001) *Proc. Natl. Acad. Sci. U. S. A.* **98,** 13554–13559

Apical Sorting of β-Secretase Limits Amyloid β-Peptide Production

Anja Capell, Liane Meyn, Regina Fluhrer, David B. Teplow, Jochen Walter and Christian Haass

J. Biol. Chem. 2002, 277:5637-5643.
doi: 10.1074/jbc.M109119200 originally published online December 6, 2001
